DMAPT inhibits NF-κB activity and increases sensitivity of prostate cancer cells to X-rays *in vitro* and in tumor xenografts *in vivo*

Marc S. Mendonca[1, 2,*], William T. Turchan[1, 2], Melanie E. Alpuche[1], Christopher N. Watson[1,5], Neil C. Estabrook[1], Helen Chin-Sinex[1], Jeremy B. Shapiro[1], Imade E. Imasuen-Williams[1], Gabriel Rangel[1], David P. Gilley[3], Nazmul Huda[2], Peter A. Crooks[4], and Ronald H. Shapiro[1,5]

[1]Departments of Radiation Oncology, Indiana University School of Medicine; Indianapolis, IN 46202 USA

[2]Medical & Molecular Genetics, Indiana University School of Medicine; Indianapolis, IN 46202 USA

[3]Department of Chemistry and Applied Sciences, South Dakota School of Mines and Technology, Rapid City, SD 57701 USA;

[4]College of Pharmacy, University of Arkansas for Medical Sciences, Little Rock, AR 72205, USA

[5]Richard L. Roudebush, VA Medical Center, Indianapolis, IN 46202 USA

[*]Correspondence and Reprint requests: Radiation & Cancer Biology Laboratories, Department of Radiation Oncology, Indiana University School of Medicine, 975 West Walnut St., IB-346, Indianapolis, IN 46202. Tel. (317) 278-0404, Fax (317) 278-0405. mmendonc@iupui.edu

Abstract

Constitutive activation of the pro-survival transcription factor NF-κB has been associated with resistance to both chemotherapy and radiation therapy in many human cancers, including prostate cancer. Our lab and others have demonstrated that the natural product parthenolide can inhibit NF-κB activity and sensitize PC-3 prostate cancers cells to X-rays *in vitro*; however,

This is the author's manuscript of the article published in final edited form as:
Mendonca, M. S., Turchan, W. T., Alpuche, M. E., Watson, C. N., Estabrook, N. C., Chin-Sinex, H., … Shapiro, R. H. (2017). DMAPT inhibits NF-κB activity and increases sensitivity of prostate cancer cells to X-rays in vitro and in tumor xenografts in vivo. Free Radical Biology and Medicine. https://doi.org/10.1016/j.freeradbiomed.2017.08.001

parthenolide has poor bioavailability *in vivo* and therefore has little clinical utility in this regard. We show here that treatment of PC-3 and DU145 human prostate cancer cells with dimethylaminoparthenolide (DMAPT), a parthenolide derivative with increased bioavailability, inhibits constitutive and radiation-induced NF-κB binding activity and slows prostate cancer cell growth. We also show that DMAPT increases single and fractionated X-ray-induced killing of prostate cancer cells through inhibition of DNA double strand break repair and also that DMAPT-induced radiosensitization is, at least partially, dependent upon the alteration of intracellular thiol reduction-oxidation chemistry. Finally, we demonstrate that the treatment of PC-3 prostate tumor xenografts with oral DMAPT in addition to radiation therapy significantly decreases tumor growth and results in significantly smaller tumor volumes compared to xenografts treated with either DMAPT or radiation therapy alone, suggesting that DMAPT might have a potential clinical role as a radiosensitizing agent in the treatment of prostate cancer.

Graphical abstract

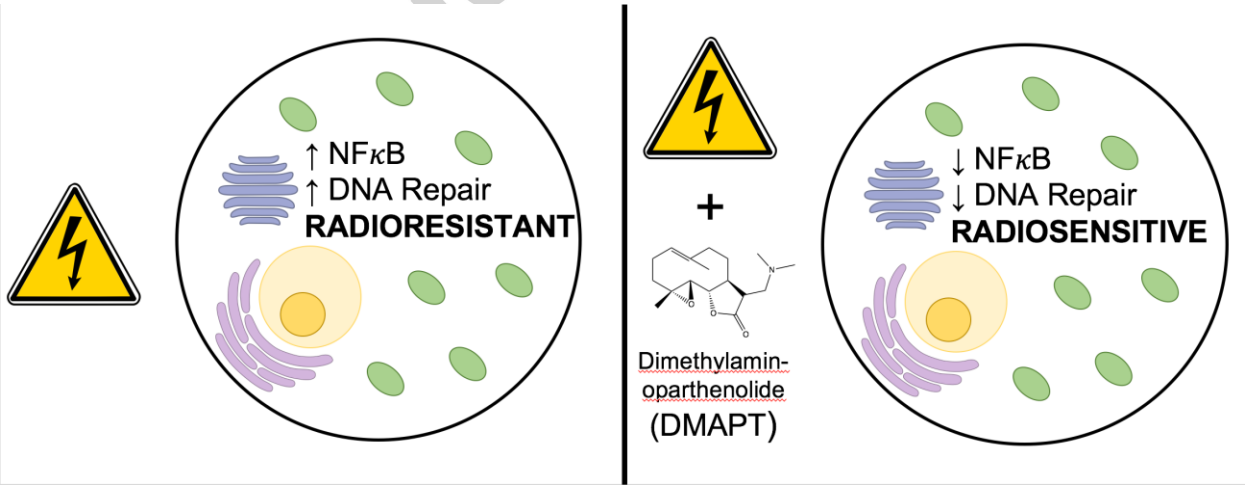

Key words: X-rays, DMAPT, NF-κB, PC-3, DU145, Split-dose repair, Comet assay, DNA double-strand break repair.

Introduction

Despite decreasing incidence over recent years, prostate cancer remains the most commonly diagnosed cancer in men, with the American Cancer Society projecting 186,890 new cases of prostate cancer in the US in 2016 (1). Moreover, the American Cancer Society estimates 26,120 men will die of prostate cancer in 2016, making it the second leading cause of cancer death in men (1). Older men diagnosed with prostate cancer tend to have a relatively good prognosis, as they are typically either successfully treated or do not succumb to the disease prior to dying of other causes (2-7). However, the prognosis of younger men and African American men diagnosed with prostate cancer, in whom the disease is often more aggressive and has the potential to metastasize earlier, is typically much worse (2-7). Thus, there remains a large need for the development of more effective treatment methods for men with prostate cancer in populations that tend to have more aggressive cancers. Although radiation therapy can be a quite effective treatment modality for patients with prostate cancer, resistance to radiation therapy and resulting local failures and reoccurrences are not uncommon; this is especially true in populations that typically have more aggressive prostate cancers (2-7).

As is the case with many cancers that are resistant to radiation therapy, radiation-resistant prostate cancer cells often overexpress the transcription factor NF-κB (8-11). Constitutive activation of NF-κB has been implicated in resistance to both radiation therapy and chemotherapy in cancer cells, and has also been shown to play a role in the stimulation of tumor cell growth, inhibition of apoptosis, and facilitation of tumor invasion, metastasis, and angiogenesis (8-17). Not only is NF-κB constitutively active in many human tumors, it is also often induced by exposure to X-rays, therefore increasing its ability to facilitate resistance to radiation therapy (10, 11, 17). Because of the ubiquity of the role played by NF-κB in resistance

to current cancer treatment modalities, the search for novel therapies that inhibit NF-κB is of great interest. One such therapy that has been studied by our lab and others is related to the naturally-occurring compound parthenolide.

Parthenolide is a naturally occurring sesquiterpene lactone that is an active ingredient in the medicinal plant *Tanacetum parthenum*, commonly known as Feverfew, which has traditionally been used as an herbal remedy for arthritis and migraine headaches (18, 19). Parthenolide has been shown to inhibit NF-κB activity by preventing the breakdown of IκB-α and IκB-β, both of which are responsible for the sequestration of NF-κB to the cytoplasm (18-24). Moreover, our lab and others have shown that parthenolide inhibits constitutive and radiation-induced NF-κB activity and human tumor xenograft growth, and enhances X-ray-induced tumor cell killing through inhibition of split-dose repair (25-28). Parthenolide has also been shown to have a variety of other anti-neoplastic actions including: activation of caspases and pro-apoptotic regulators such as BAX, induction of reactive oxygen species and apoptosis-related transcription factors such as GADD153, and alteration of cell cycle distributions via the cyclin-dependent kinase inhibitor $p21^{waf\text{-}1/cip1}$ (18, 19, 25-31). Moreover, parthenolide-induced apoptosis has also shown to be significantly mediated by depletion of intracellular thiols (32).

Despite its anti-neoplastic properties, parthenolide unfortunately has a rather low bioavailability, which limits its clinical utility (33). In one study, human volunteers were given up to 4 mg of *Tanacetum parthenum* extract orally with no detectable parthenolide in the plasma (<0.5ng/mL) (33). As a remedy for this problem, a derivative of parthenolide, dimethylaminoparthenolide (DMAPT), which has a much higher oral bioavailability than parthenolide, has been developed (28,34-38). In a mouse model, 100 mg/kg of oral DMAPT

produced a maximum serum concentration of 25 μM, compared to a maximum possible serum concentration of 0.2 μM with oral parthenolide (34).

Like parthenolide, DMAPT, has been shown to be a potent inhibitor of NF-κB. Previous work in our lab showed that DMAPT inhibited NF-κB activity in non-small cell lung cancer cells and sensitized these cells to X-rays (28). There is evidence that DMAPT promotes prostate cancer cell death *in vivo* via both inhibition of NF-κB activity and generation of reactive oxygen species (ROS) (34). Moreover, very recent work by Morel *et al* demonstrated the ability of parthenolide and DMAPT to radiosensitize prostate cancer cells *in vivo* in a transgenic adenocarcinoma of the mouse prostate (TRAMP) model while acting as a radioprotecting agent in normal tissue (39). While these studies give us additional insight into the ability of DMAPT to induce radiosensitization, there is still relatively little data on the mechanism of DMAPT-induced radiosensitization in human prostate cancer cells. Given that the α-methylene-γ-lactone group of parthenolide, which is altered in DMAPT, contributes to the ability of parthenolide to act as a thiol alkylating agent and deplete intracellular thiols, it is reasonable to question whether the radiosensitizing effects of DMAPT are dependent upon its ability to react with biological thiols (40). Moreover, given our evidence that DMAPT-induced X-ray sensitivity of lung cancer occurs, at least partially, via the inhibition of split-dose repair (28), we investigated whether DMAPT is capable of significantly increasing the sensitivity of prostate cancer to X-rays through this mechanism, and thus our work here was aimed at answering these questions. Our results show that treatment of PC-3 (p53 null) and DU145 (p53 mutant) human prostate cancer cells with DMAPT inhibits NF-κB activity, cell growth, and DNA double strand break repair; and increases radiation-induced cell killing of single and fractionated X-ray treatments of PC-3 and DU145 cells *in vitro,* and of a single fraction of X-rays given to PC-3 tumor xenografts *in vivo*.

Moreover, our results show that pre-treatment with the thiol antioxidant N-acetylcysteine (NAC), reduced, but did not completely eliminate the enhanced radiation-induced cell killing seen in cells treated with DMAPT, suggesting that DMAPT-induced radiosensitization is partially dependent on its ability to interact with biological thiols.

Materials and Methods

Cell lines

PC-3 is a p53 null, human androgen-independent prostate cancer cell line that was obtained from Dr. Tom Gardner, Indiana University School of Medicine (41). DU145 is a p53 mutated, human hormone-insensitive prostate adenocarcinoma cell line originally isolated from a brain metastasis that was also obtained from Dr. Tom Gardner, Indiana University School of Medicine (42-44). Neither PC-3 nor DU145 express androgen receptors (AR) or prostate specific antigen (PSA). The cells were grown in Roswell Park Memorial Institute (RPMI) 1640 medium with L-glutamine (Thermo Fisher Scientific, Waltham, MA), 10% FBS (Hyclone, Logan, UT), and 1% penicillin/streptomycin (Cellgro, Herndon VA). Cells were cultured at 37°C, 5% CO_2, and 85% humidity. Subconfluent stock cultures plated at 6.0 x 10^5 cells were grown in T-75 tissue culture flasks 1 to 3 days prior to all experiments. The PC-3 *in vitro* population doubling time and plating efficiency were 23 ± 5 h and 35 ± 5%, respectively. The DU145 *in vitro* population doubling time and plating efficiency were 20.4 ± 2.2 h and 45 ± 8%, respectively.

Assessment of constitutive NF-κB binding activity, plating efficiency, apoptosis, cell cycle distribution and cell growth in PC-3 and DU145 cells

Dimethylaminoparthenolide (DMAPT) was synthesized by Dr. Peter Crooks and is a derivative of parthenolide, a sesquiterpene lactone, extracted from the Feverfew plant (28, 34-38). PC-3 and DU145 cells were harvested from exponentially growing stock cultures and plated in T-25 flasks (Corning, Corning, NY). Twenty-four and forty-eight hours after plating, appropriate volumes of 36 mM DMAPT drug stock diluted in RPMI were directly added to the cell culture flasks so that final DMAPT concentrations were 0, 2.5, and 5 μM DMAPT for PC-3 and 0 and 4 μM DMAPT for DU145 cells. Control and treated cells were harvested for NF-κB EMSA/Gel shifts, cell counting/growth curve analysis, clonogenic potential/plating efficiency studies, flow cytometry based apoptosis analysis by Annexin V-phosphatidylserine analysis, comet assays to determine DNA double strand break repair, flow cytometry based DNA histogram cell cycle analysis after propidium iodide staining, and Western analyses 24 and 48 hours after drug addition by our standard techniques (12, 26, 28, 45, 46). Since the initial NF-κB EMSA/Gel shifts clearly showed better inhibition of NF-kB binding at 5 μM DMAPT, all other experiments with PC-3 were performed at 5 μM DMAPT.

Electrophoretic mobility shift assay (EMSA)

PC-3 cells were treated with 0 or 5 μM of DMAPT and DU145 cells were treated with 0 or 4 μM of DMAPT at 24 and 48 hours as described above and then cell extracts were harvested by scraping flasks on ice for NF-κB EMSA/Gel Shift analysis by our standard methods described previously (12, 26, 28). The NF-κB oligonucleotide, 5'-AGTTGAGGGGACTTTCCCAGG-3', containing the NF-κB DNA binding consensus sequence (Promega, Madison, WI) was T4 kinase end-labeled with ^{32}P (Perkin Elmer, Waltham, MA) and was utilized for all studies.

Western blots

Twenty-four and forty-eight hours after treatment of PC-3 and DU145 cells with 0 or 5 μM of DMAPT, or 0 or 4 μM of DMAPT, respectively, cells were analyzed for changes in protein expression by our standard Western analysis (26, 28, 46). The primary antibodies utilized were anti-p53 (Ab-6, Calbiochem and clone BP53-12 Upstate), anti-p73 (rabbit polyclonal, Chemicon), anti-$p21^{waf\text{-}1/Cip\text{-}1}$ (clone 6B6, BD Pharmingen and mixed monoclonal, Upstate), anti-Bax (Clone YTH-2D2, Trevigen), anti-Bcl-2 (clone 124, Dako), anti-Bid (BD Pharmingen), and anti-α-tubulin (cloneB-5-1-2, Sigma). The membranes were incubated with appropriate secondary antibodies conjugated with peroxidase (Pierce, Rockford, IL).

Single fraction X-ray survival studies with and without DMAPT

All X-ray *in vitro* studies of PC-3 and DU145 cells were conducted using a 160 kV Faxitron X-ray Machine (Faxitron Bioptics, Tucson, AZ). Settings for the Faxitron X-ray machine were 0.5 mm Cu filter, d=33 cm, and dose rate 62.8 cGy/min. X-ray dosimetry was performed according to the AAPM Task Group 61 protocol using a PTW N300001 ion chamber and an electrometer calibrated by the University of Wisconsin Accredited Dosimetry Calibration Laboratory (UW-ADCL) (47, 48). PC-3 cells were treated with 0 and 5 μM DMAPT. DU145 cells were treated with 0 or 4 μM of DMAPT. After incubation for 24 hours with DMAPT the PC-3 and DU145 cells were treated with a second dose of 5 or 4 μM DMAPT, respectively, and then were irradiated with a single dose of between 0 and 6 Gy of 160 kVp X-rays. After an additional 24 h for repair, both PC-3 and DU145 cells were trypsinized; single cell suspensions were then prepared and counted. At each X-ray dose, appropriate numbers of cells were then

plated into six T-25 flasks for standard colony forming assays by our published methods to assess clonogenic capacity/plating efficiency and survival (26, 28, 48, 49). As previously stated, the surviving fractions after various X-ray doses and DMAPT treatments were normalized for the toxicity of DMAPT alone. This was done to distinguish enhancement of radiation-induced cell killing from merely additive toxicity of the drug and radiation (26, 28). The Surviving Fraction (SF) mean ± SD of the radiation-alone versus the SF mean ± SD observed with DMAPT and radiation were compared by the Student's *t*-test for significance ($P \leq 0.05$). Each experiment was performed a minimum of six times.

Single fraction X-ray survival studies of cells pre-treated with NAC prior to DMAPT treatment

In order to better determine the mechanism of DMAPT-mediated radiosensitization, studies were performed in both the PC-3 and DU145 cells lines with pre-treatment of the cells with NAC prior to DMAPT treatment and radiation. PC-3 and DU145 cells in the NAC-pre-treatment group were treated with 20 mM NAC for 4 hours and were then washed with PBS. Cells were then treated with DMAPT immediately and 24 hours later, irradiated with a single dose of between 0 and 6 Gy of 160 kVp X-rays, and plated to assess clonogenic capacity/plating efficiency and survival in the aforementioned manner (26, 28, 48, 49).

Immediate plating and split-dose repair experiments

A control group and five experimental groups were used for both PC-3 and DU145 cell immediate plating and split-dose repair experiments. The five experimental conditions were:

DMAPT only (5 or 4 μM, for PC-3 or DU145, respectively), 4 Gy with immediate plating, 4 Gy with DMAPT (5 or 4 μM, for PC-3 or DU145, respectively) and immediate plating, and 2 x 2 Gy split-dose group with or without DMAPT treatment (5 or 4 μM, for PC-3 or DU145, respectively). For both PC-3 and DU145 2 X 2 Gy split-dose groups a 4-hour incubation at 37°C was present between the two 2 Gy treatments to allow for repair. Cells were irradiated on ice to prevent repair during the treatments (26, 28).

Comet assay

To investigate whether DMAPT altered the repair of X-ray-induced DNA double strand breaks (DSBs), neutral comet assays were performed using CometAssay™ kits (Trevigen 4252-040-K) employing our standard methodology (28). PC-3 and DU145 cells were treated with 0 or 5 μM, or 0 or 4 μM DMAPT, respectively at 24 and 48 hours. After the second DMAPT treatment, cells were irradiated at 20 Gy of 160 kVp X-rays. To monitor DSB rejoining, cells were placed at 37ºC for 0 to 24-hour incubation periods and then at select times trypsinized, washed with PBS, embedded in agarose, lysed and subjected to neutral gel electrophoresis. Immediately before image analysis, cells were treated with SYBR green (Thermo Fisher Scientific). The cells were examined using a Leica CTR 5000 fluorescent microscope (Lecia Microsystems, Wetzlar, Germany) and comet images were captured using the SPOT RT™ software (SPOT Imaging Solutions, Sterling Heights, MI). The comet tail moments (50, 51) were analyzed by TriTekCometScore Freeware program (www.autocomet.com). Average tail moment values versus incubation times after 20 Gy of X-rays were calculated by measuring the tail moments of at least 100 cells per sample.

Protocol for in vivo study in nude mice

In vivo PC-3 tumor xenograft studies were carried out with athymic nude mice (Envigo, Indianapolis, IN). In accordance with our standard procedure, mice were injected subcutaneously with between 5 and 10 million PC-3 cells in the right flank; tumors were then allowed to grow for seven days (28, 48). The PC-3 tumor xenografts were then randomly assigned to either the control or one of three treatment groups: DMAPT only, 4 Gy only, or DMAPT plus 4 Gy. Beginning on day 8 post-subcutaneous injection, the mice in the control group were given 2.5% mannitol by oral gavage, while the DMAPT-treated groups were given 100 mg/kg DMAPT in 2.5% mannitol daily for 7 days. The tumor xenografts in the irradiated groups were irradiated with a single fraction of 4 Gy with a 320 Precision X-ray Machine (Precision X-ray, North Bradford, CT) using a collimated 2.0 x 2.0 cm field size that focused the radiation treatment on the tumor and minimized the amount of normal tissue irradiated. The mice in the DMAPT with 4 Gy treatment group received the 4 Gy dose of X-rays on the third day after the DMAPT treatment began. Settings for the Precision X-ray machine were 250 kVp, 2.0 mm Cu/Th filter, d= 50 cm, and dose rate 1.59 Gy/min. All animal experiments were conducted under an approved Indiana University School of Medicine IUACUC protocol in our fully ALAC accredited IUSOM animal facility.

Statistical analyses

The Surviving Fraction (SF) means ± SD of the radiation-alone versus the SF means ± SD observed with DMAPT and radiation for the above single fraction and split-dose clonogenic survival experiments were compared by the Student's *t*-test for significance ($P \leq 0.05$). The Comet Tail Moments (50, 51) means for each time point for radiation-alone versus radiation and DMAPT were compared by the Student's *t*-test for significance ($P \leq 0.05$). Each *in vitro* experiment was performed four to six times. For the PC-3 tumor xenograft studies, tumor volume was measured in each xenograft on day 8 post-injection. Tumor volume was subsequently measured at intervals of 2-4 days up until day 59 post-injection. Using the originally measured tumor volume on day 8 post-injection, the relative tumor volume was determined on each day of measurement for each of the xenografts. This data was compiled to determine the average relative tumor volume for each of the four groups on each day of measurement. The average relative tumor volume in each group was then used to create a tumor growth curve and a one-way ANOVA was performed to determine the statistical significance of the relative tumor volume on each day of measurement.

Results

DMAPT decreases constitutive NF-κB binding activity, inhibits cell proliferation and viability of PC-3 and DU145 cells

Electrophoretic Mobility Shift Assays (EMSA) were performed to investigate whether treatment of PC-3 or DU145 prostate cancer cells with DMAPT altered the binding affinity of the p65/p50 heterodimer of NF-κB to its DNA promoter consensus sequence in either cell type. Treatment of PC-3 and DU145 cells with 5 and 4 μM DMAPT, respectively, for 48 hours

reduced binding activity of the NF-κB p65/p50 heterodimer transcription factors in both cell lines (Figs. 1A & 1B, left panels). In addition, treatment of PC-3 and DU145 cells with 5 and 4 μM DMAPT, respectively, increased the population doubling times of PC-3 prostate cancer cells from 23.0 ± 5.0 hours to 42.0 ± 3.0 hours and of the DU145 cells from 20.4 ± 2.2 hours to 72.5 ± 24.8 hours (Figs. 1A & 1B, right upper panels) ($P < 0.05$). Clonogenic survivals were performed to establish plating efficiencies and determine if the increased doubling times in PC-3 and DU145 cells could in part be due to induction of cell death by DMAPT. Treatment with DMAPT for 48 hours significantly decreased the clonogenic plating efficiency of PC-3 cells from 0.31 ± 0.07 to 0.14 ± 0.05 ($P < 0.05$) and reduced the clonogenic plating efficiency of DU145 cells from 0.45 ± .08 to 0.22 ± 0.07 ($P < 0.05$), indicating that cell death does appear to play a role in the observed increase in cell population doubling time following treatment with DMAPT (Figs. 1A & 1B, right lower panels). However, analysis of whether the DMAPT treated cells are dying by apoptosis by Annexin V flow cytometry indicates no significant difference in the percentage of cell undergoing apoptosis in either PC-3 or DU145 cells that were treated with DMAPT versus the untreated control cells (Figs. 2A & 2B, left panels). Moreover, Western blots show no obvious evidence of induction of pro-apoptotic or anti-apoptotic BCL proteins such as Bax, Bcl-2, or Bid (Figs. 2A & 2B, right panels). These data indicate that the increased cell death observed after the treatment of PC-3 and DU145 cells with DMAPT cannot be explained by the induction of apoptosis.

DMAPT reduces radiation-induced NF-κB binding activity and increases radiation-induced cell killing of PC-3 and DU145 cells

The binding activity of the p65/p50 heterodimer of NF-κB to its consensus promoter sequence has been shown by us and other investigators to be X-ray-inducible and associated with radiation resistance (10, 11, 17). We therefore performed NF-κB EMSA gel shift studies to investigate whether treatment of PC-3 or DU145 cells with DMAPT altered the kinetics or intensity of radiation-induced NF-κB activation in PC-3 and DU145 cells. PC-3 and DU145 cells were irradiated with 6 Gy and nuclear extracts were obtained from irradiated cultures of PC-3 and DU145 cells treated with and without DMAPT at 0, 15, 30, 45, and 60 minutes post-irradiation. Radiation-induced NF-κB binding activity in PC-3 cells was elevated from 15 to 45 minutes after 6 Gy, and treatment with DMAPT completely inhibited radiation-induced NF-κB binding activity in PC-3 cells (Fig. 3A). Radiation-induced NF-κB binding activity in DU145 cells was elevated from 30 to 60 minutes after 6 Gy, and treatment with DMAPT reduced but did not completely suppress radiation-induced NF-κB binding activity in DU145 cells (Fig. 3B).

To test whether treatment of PC-3 or DU145 cells with DMAPT would alter radiation-induced cell killing, PC-3 and DU145 cells were treated for 48 hours with or without DMAPT, irradiated with a single dose of X–rays in the range of 0 to 7 Gy, incubated for another 24 hours with or without DMAPT, and then plated for colony formation. DMAPT treatment increased X-ray-induced cell killing compared to irradiated controls at 2, 4, and 6 Gy in PC-3 cells and at 3, 4, 5, 6, and 7 Gy in DU145 cells (Fig. 4, upper panel) ($P < 0.05$). It should be noted that the calculated cell survivals of the DMAPT-treated PC-3 and DU145 cells have been corrected for drug-related toxicity and therefore toxicity related to DMAPT cannot account for the enhanced X-ray-induced cell killing that was observed.

Treatment with NAC reduces DMAPT-induced radiosensitization of PC-3 and DU145 cells

To test whether pre-treatment with NAC reduced the enhanced radiation-induced cell killing seen in cells treated with DMAPT, PC-3 and DU145 cells were treated with NAC for 4 hours prior to washing and then treating the cells with DMAPT immediately and 24 hours later and then irradiating them. In both the PC-3 and DU145 cell lines pre-treatment with NAC significantly reduced, but did not eliminate, the enhanced radiation-induced cell killing of cells treated with DMAPT and 6 Gy of X-rays (Fig. 4, lower panel) ($P < 0.05$).

DMAPT alters cell cycle distribution

Flow cytometry was then performed to investigate whether altered cell cycle distribution out of the radiation resistant S phase or into the radiation sensitive G2/M phase could explain the DMAPT-induced radiosensitization of p53 null PC-3 or DU145 prostate cancer cells. Flow cytometry indicated that while DMAPT treatment of PC-3 cells did increase the number of cells in the radiation sensitive G_2/M phase from 18% to 27%, it also increased the number of radiation resistant S phase cells increasing from 38% to 54% (Fig. 5A). As previously mentioned, Western blot analysis confirmed that PC-3 was p53 null and showed that DMAPT did not induce $p21^{waf1/cip1}$, a powerful inhibitor of the cell cycle progression at multiple cell cycle check points (Fig. 2). Therefore, the observed changes in the cell cycle induced by DMAPT treatment appear not to be a function of p53 activation and subsequent up-regulation of $p21^{waf1/cip1}$. By contrast, flow cytometric assessment of alterations of cell cycle in DMAPT treated DU145 cells did not show an increase in the percentage of radiation-sensitive cells in G_2/M phase, but it too showed an increase in the number of radiation-resistant cells in S phase from 30% to 55% (Fig. 5B). Taken together the data suggest that the observed increase in X-ray sensitivity of PC-3 and

DU145 cells after treatment with DMAPT cannot be explained by redistribution of the cells into radiation sensitive phases of the cell cycle.

DMAPT inhibits split-dose repair and enhances fractionated x-ray-induced cell killing

X-ray fractionation studies were performed to investigate whether DMAPT increased radiation-induced killing of PC-3 and DU145 cells through inhibition of split-dose repair. The surviving fraction of PC-3 cells that were treated with 0 or 5 μM DMAPT or DU145 cells treated with 0 or 4 μM DMAPT were then given either a single fraction of 4 Gy of X-rays or two fractions of 2 Gy of X-rays 2 hours apart to allow for repair. The data show that the survival fractions of both PC-3 and DU145 cells treated with DMAPT and 2 Gy + 2 Gy fractionated radiation were significantly lower than the surviving fractions of PC-3 and DU145 cells that were treated with 2 Gy + 2 Gy fractionated radiation alone (Fig. 6A) ($P < 0.01$).

DMAPT inhibits DNA double-strand break repair in irradiated PC-3 and DU145 prostate cancer cells

To directly investigate whether the above inhibition of split dose repair by DMAPT treatment was due to inhibition of DNA double-strand break repair, flasks of PC-3 (left) and DU145 (right) cells were irradiated with 20 Gy of X-rays on ice with and without treatment with DMAPT and samples at various time points post-irradiation were prepared for neutral comet assay, which assesses both radiation-induced DNA double-strand break (DSB) induction and repair (50-52). The mean ± s.d. Comet olive tail moments for 50 individual cells from each treatment group of PC-3 and DU145 cells were determined and plotted versus time post-irradiation (6B, lower panels). The 20 Gy control comet data for both PC-3 and DU145 clearly show evidence of the

classic fast and slow bimodal repair kinetics versus time post-irradiation that has been reported by us and other investigators (50, 51, 53, 54). The data also show that treatment with DMAPT results in significantly longer tail moments (i.e. less DSB repair) in irradiated PC-3 cells at 1, 3, and 6 hours post-irradiation and in irradiated DU145 cells at 3, 6, and 14 hours post-irradiation compared to the results from 20 Gy irradiated control PC-3 and DU145 cells (Fig. 6B, lower panels) ($P < 0.05$). The data indicate that treatment with DMAPT alters the fast and slow components of DNA DSB repair post-irradiation in both PC-3 and DU145 cells. We and others have shown that altered radiation-induced DSB repair kinetics post-irradiation is strongly correlated with increased radiation-induced cell death in mammalian cells (50, 51, 53, 54).

Treatment with DMAPT increases sensitivity of PC-3 tumor xenografts to X-rays

PC-3 tumor xenograft studies were performed to determine whether DMAPT increases sensitivity of PC-3 cells to X-rays *in vivo*. Treatment of xenografts with the combination of DMAPT and 6 Gy of X-rays resulted in significantly lower average relative tumor volumes on day 59-post-implantation compared to xenografts that were untreated or treated with either DMAPT or 6 Gy of X-rays alone (Fig. 7) ($P < 0.05$).

Discussion

Previous work in our laboratory has shown that parthenolide, a naturally occurring sesquiterpene lactone, is a potent radiosensitizing agent that is effective at increasing the sensitivity of the human prostate adenocarcinoma cell line PC-3 to X-rays *in vitro* (26, 27). However, given its poor bioavailability, the clinical utility of parthenolide as a radiosensitizing

agent is limited (33). Thus, we investigated whether DMAPT, a derivative of parthenolide with increased bioavailability, would be able to increase the sensitivity of not only PC-3 (p53 null) but also DU145 (p53 mutant) prostate cancer cells to X-rays *in vitro* and *in vivo* (28, 35-38).

Treatment of PC-3 cells with 5 μM DMAPT at 24 and 48 hours reduced constitutive NF-κB activation (Fig. 1A, left panel), inhibited cell growth, and reduced plating efficiency (Fig. 1A, right lower panel). The increased cell population doubling time observed in PC-3 cells that were treated with DMAPT (Fig. 1A, right upper panel) is consistent with the growth inhibition seen in this cell line when treated with parthenolide (26, 27). While the increase in doubling time observed following treatment with DMAPT might be explained by an increase in cell death, Annexin V flow cytometry assays showed that DMAPT treatment did not increase apoptosis in PC-3 cells (Fig. 2A, left panel). Moreover, Western blot results showed that DMAPT did not change the expression of pro- or anti-apoptotic proteins (Fig 2A, right panel). Taken together, these results suggest that apoptosis is not responsible for the increased cell killing seen in DMAPT-treated PC-3 cells. These studies were also performed using DU145 prostate adenocarcinoma cells, which similarly showed reduced constitutive NF-κB activation, increased doubling time, and reduced plating efficiency that could not be explained by apoptosis following treatment with DMAPT (Figs. 1B and 2B).

PC-3 cells have been found to express NF-κB constitutively and in response to ionizing radiation (7). Thus, we investigated whether DMAPT would decrease radiation-induced NF-κB binding in PC-3 cells. We found that treatment of PC-3 cells with DMAPT completely inhibited radiation-induced NF-κB binding in this cell line (Fig. 3A). While this effect was not as pronounced in the DU145 cell line (Fig. 3B), DMAPT increased X-ray-induced cell killing in both PC-3 and DU145 cell lines (Fig. 4, upper panel).

As previously mentioned, parthenolide is known to be a potent thiol alkylating agent and is known to exert an anti-neoplastic effect via this mechanism. However, given that the α-methylene-γ-lactone group of parthenolide has been modified in DMAPT in order to increase the drug's bioavailability, it is relatively unknown whether the aforementioned DMAPT-induced radiosensitization is mediated via the alteration of intracellular thiol reduction-oxidation chemistry (32, 40). As such, we performed experiments to test whether pre-treatment with the thiol antioxidant NAC would inhibit the ability of DMAPT to radiosensitive PC-3 and DU145 cells. Our results showed that while pre-treatment with NAC significantly decreased the degree of radiosensitization seen in both cell lines following treatment with DMAPT, it did not completely eliminate this effect. Thus, this novel finding provides evidence that although some of the DMAPT-induced radiosensitization seen in these cell lines is due to alterations in intracellular thiol reduction-oxidation chemistry, these alterations alone are not sufficient to explain the mechanism of DMAPT-induced radiosensitization.

In an additional attempt to explain the radiosensitization seen in PC-3 and DU145 cells following treatment with DMAPT, cell cycle analysis was utilized. We found that while treatment with DMAPT resulted in a small increase in the number of PC-3 cells in the radiosensitive G_2/M phase, it also resulted in an even larger increase in the number of cells in the radioresistant S phase (Fig. 5A). Similarly, we found that DMAPT had no effect on the number of DU145 cells in the radiosensitive G_2/M phase and resulted in a significant increase in the number of cells in the radioresistant S phase. Thus, our results indicate that DMAPT-induced radiosensitization does not occur because of cell cycle changes in either of these cell lines.

In a further effort to understand DMAPT's role as a radiosensitizing agent, we also performed split-dose experiments in which DMAPT-treated and untreated cells were irradiated

with 4 Gy of X-rays, either in a single fraction or in two fractions of 2 Gy. We found that the surviving fraction of PC-3 cells that were treated with DMAPT combined with two fractions of 2 Gy of X-rays was significantly lower than the surviving fraction of PC-3 cells that were treated with DMAPT combined with a single fraction of 4 Gy of X-rays, or with radiation alone (Fig. 6A, left panel). Although these results could not be replicated in DU145 cells (Fig. 6A, right panel), our results in the PC-3 cell line suggest that treatment with DMAPT might decrease cell survival by impairing the ability of these cells to repair radiation-induced double strand DNA breaks. This idea is supported by the results of the comet assays, in which significantly larger tail moments, created by double stranded DNA fragments, were detected in PC-3 cells that were treated with a combination of DMAPT and radiation compared with those that were treated with radiation alone (Fig. 6B). overall, these data support the idea that DMAPT-mediated inhibition of radiation-induced NF-κB expression inhibits DNA double strand break repair, and is at least partially responsible for the effectiveness of DMAPT as a radiosensitizing agent in PC-3 prostate adenocarcinoma cells, further studies to identify the molecular mechanisms involved are underway.

Finally, we have demonstrated that DMAPT is effective as a radiosensitizing agent *in vivo* in a nude mouse model. PC-3 tumor xenografts that were treated with oral DMAPT at 100 mg/kg daily for 7 days combined with 6 Gy of X-rays had significantly smaller tumor volumes compared to xenografts that were untreated, or treated with either DMAPT or radiation alone (Fig. 7). Very recent work by Morel *et al* showed that DMAPT is able to radiosensitize prostate cancer cells *in vivo* in a transgenic adenocarcinoma of the mouse prostate (TRAMP) model (39). This work provides further support for our conclusion that DMAPT is able to radiosensitize prostate cancer cells *in vivo*. Moreover, the finding by Morel *et al* that DMAPT also acts as a

radioprotecting agent in normal tissues *in vivo* increases the future potential for DMAPT as a therapeutic and radiosensitizing agent for prostate cancer (39).

Although current therapeutic regimens offer a favorable prognosis for many older men with prostate cancer, the disease remains the second most common cause of cancer death in men, primarily as a result of the poor prognosis the disease portends in younger men, and African American men (1-7). To improve the prognosis of prostate cancer in these populations new therapeutic paradigms are necessary. Based upon our findings herein, we believe that DMAPT has the potential to be used clinically as a radiosensitizing agent in the treatment of prostate cancer. Moreover, further investigations should be undertaken to evaluate DMAPT as a radiosensitizing agent in other malignancies where NF-κB is activated, as our lab has done previously with non-small cell lung cancer (28).

Disclosures

All authors except PAC have nothing to disclose. PAC owns stock in the company Leuchemix developing the parthenolide derivative DMAPT for clinical use.

Acknowledgments

MSM thanks the Department of Radiation Oncology and the IU Simon Cancer Center Summer Research Program, Indiana University School of Medicine for financial support for these studies. WTT and MSM acknowledge the support of the NIH T35HL110854 training grant. PAC acknowledges support from NIH/NCI grant R01 CA158275.

References

1. ACS. Cancer Facts & Figures . American Cancer Society. 2016.

2. Lawton CA, Winter K, Grignon D, Pilepich MV. Androgen suppression plus radiation versus radiation alone for patients with stage D1/pathologic node-positive adenocarcinoma of the prostate: updated results based on national prospective randomized trial Radiation Therapy Oncology Group 85-31. J Clin Oncol. 2005;23(4):800-7.

3. Thoms J, Goda JS, Zlotta AR, Fleshner NE, van der Kwast TH, Supiot S, et al. Neoadjuvant radiotherapy for locally advanced and high-risk prostate cancer. Nature reviews Clinical oncology. 2011;8(2):107-13.

4. Johung K, Saif MW, Chang BW. Treatment of locally advanced pancreatic cancer: the role of radiation therapy. International journal of radiation oncology, biology, physics. 2012;82(2):508-18.

5. Ramey SJ, Marshall DT, J. Re-irradiation for salvage of prostate cancer failures after primary radiotherapy. World. 2012.

6. Rischke HC, Knippen S, Kirste S, Grosu AL. Treatment of recurrent prostate cancer following radical prostatectomy: the radiation-oncologists point of view. The quarterly journal of nuclear medicine and molecular imaging : official publication of the Italian Association of Nuclear Medicine (AIMN) [and] the International Association of Radiopharmacology (IAR), [and] Section of the Society of. 2012;56(5):409-20.

7. Parekh A, Graham PL, Nguyen PL. Cancer control and complications of salvage local therapy after failure of radiotherapy for prostate cancer: a systematic review. Seminars in radiation oncology. 2013;23(3):222-34.

8. Nakshatri H, Bhat-Nakshatri P, Martin DA, Goulet RJ, Sledge GW. Constitutive activation of NF-kappaB during progression of breast cancer to hormone-independent growth. Molecular and cellular biology. 1997;17(7):3629-39.

9. Lindholm PF, Bub J, Kaul S, Shidham VB, Kajdacsy-Balla A. The role of constitutive NF-kappaB activity in PC-3 human prostate cancer cell invasive behavior. Clinical & experimental metastasis. 2000;18(6):471-9.

10. Jung M, Dritschilo A. NF-kappa B signaling pathway as a target for human tumor radiosensitization. Seminars in radiation oncology. 2001;11(4):346-51.

11. Karin M, Cao Y, Greten FR, Li Z-W. NF-kappaB in cancer: from innocent bystander to major culprit. Nature reviews Cancer. 2002;2(4):301-10.

12. Sweeney C, Li L, Shanmugam R, Bhat-Nakshatri P, Jayaprakasan V, Baldridge LA, et al. Nuclear factor-kappaB is constitutively activated in prostate cancer in vitro and is overexpressed in prostatic intraepithelial neoplasia and adenocarcinoma of the prostate. Clinical cancer research : an official journal of the American Association for Cancer Research. 2004;10(16):5501-7.

13. Kim HJ, Hawke N, Baldwin AS. NF-kappaB and IKK as therapeutic targets in cancer. Cell death and differentiation. 2006;13(5):738-47.

14. Habraken Y, Piette J. NF-kappaB activation by double-strand breaks. Biochemical pharmacology. 2006;72(9):1132-41.

15. Arlt A, Gehrz A, Müerköster S, Vorndamm J, Kruse M-L, Fölsch UR, et al. Role of NF-kappaB and Akt/PI3K in the resistance of pancreatic carcinoma cell lines against gemcitabine-induced cell death. Oncogene. 2003;22(21):3243-51.

16. Magne N, Toillon RA, Bottero V, Didelot C, Houtte PV, Gerard JP, et al. NF-kappaB modulation and ionizing radiation: mechanisms and future directions for cancer treatment. Cancer Lett. 2006;231(2):158-68.

17. Criswell T, Leskov K, Miyamoto S, Luo G, Boothman DA. Transcription factors activated in mammalian cells after clinically relevant doses of ionizing radiation. Oncogene. 2003;22(37):5813-27.

18. Pareek A, Suthar M, Rathore GS, Bansal V. Feverfew (Tanacetum parthenium L.): A systematic review. Pharmacognosy reviews. 2011;5(9):103-10.

19. Kreuger MRO, Grootjans S, Biavatti MW, Vandenabeele P, D'Herde K. Sesquiterpene lactones as drugs with multiple targets in cancer treatment: focus on parthenolide. Anti-cancer drugs. 2012;23(9):883-96.

20. Bork PM, Schmitz ML, Kuhnt M, Escher C, Heinrich M. Sesquiterpene lactone containing Mexican Indian medicinal plants and pure sesquiterpene lactones as potent inhibitors of transcription factor NF-kappaB. FEBS letters. 1997;402(1):85-90.

21. Hehner SP, Hofmann TG, Dröge W, Schmitz ML. The antiinflammatory sesquiterpene lactone parthenolide inhibits NF-kappa B by targeting the I kappa B kinase complex. Journal of immunology (Baltimore, Md : 1950). 1999;163(10):5617-23.

22. Heptinstall S, Groenewegen WA, Spangenberg P, Lösche W. Inhibition of platelet behaviour by feverfew: a mechanism of action involving sulphydryl groups. Folia haematologica (Leipzig, Germany : 1928). 1988;115(4):447-9.

23. Ichikawa H, Nakamura Y, Kashiwada Y, Aggarwal BB. Anticancer drugs designed by mother nature: ancient drugs but modern targets. Current pharmaceutical design. 2007;13(33):3400-16.

24. Nam N-H. Naturally occurring NF-kappaB inhibitors. Mini reviews in medicinal chemistry. 2006;6(8):945-51.

25. Sun Y, St Clair DK, Fang F, Warren GW, Rangnekar VM, Crooks PA, et al. The radiosensitization effect of parthenolide in prostate cancer cells is mediated by nuclear factor-kappaB inhibition and enhanced by the presence of PTEN. Molecular cancer therapeutics. 2007;6(9):2477-86.

26. Mendonca MS, Chin-Sinex H, Gomez-Millan J, Datzman N, Hardacre M, Comerford K, et al. Parthenolide sensitizes cells to X-ray-induced cell killing through inhibition of NF-kappaB and split-dose repair. Radiation research. 2007;168(6):689-97.

27. Watson C, Miller DA, Chin-Sinex H, Losch A, Hughes W, Sweeney C, et al. Suppression of NF-kappaB activity by parthenolide induces X-ray sensitivity through inhibition of split-dose repair in TP53 null prostate cancer cells. Radiation research. 2009;171(4):389-96.

28. Estabrook NC, Chin-Sinex H, Borgmann AJ, Dhaemers RM, Shapiro RH, Gilley D, et al. Inhibition of NF-κB and DNA double-strand break repair by DMAPT sensitizes non-small-cell lung cancers to X-rays. Free radical biology & medicine. 2011;51(12):2249-58.

29. Wen J, You K-R, Lee S-Y, Song C-H, Kim D-G. Oxidative stress-mediated apoptosis. The anticancer effect of the sesquiterpene lactone parthenolide. The Journal of biological chemistry. 2002;277(41):38954-64.

30. Pozarowski P, Halicka DH, Darzynkiewicz Z. Cell cycle effects and caspase-dependent and independent death of HL-60 and Jurkat cells treated with the inhibitor of NF-kappaB parthenolide. Cell cycle (Georgetown, Tex). 2003;2(4):377-83.

31. Pozarowski P, Halicka DH, Darzynkiewicz Z. NF-kappaB inhibitor sesquiterpene parthenolide induces concurrently atypical apoptosis and cell necrosis: difficulties in

identification of dead cells in such cultures. Cytometry Part A : the journal of the International Society for Analytical Cytology. 2003;54(2):118-24.

32. Zhang S, Ong CN, Shen HM. Critical roles of intracellular thiols and calcium in parthenolide-induced apoptosis in human colorectal cancer cells. Cancer Lett. 2004; 208(2):143-53.

33. Curry EA, Murry DJ, Yoder C, Fife K, Armstrong V, Nakshatri H, et al. Phase I dose escalation trial of feverfew with standardized doses of parthenolide in patients with cancer. Investigational new drugs. 2004;22(3):299-305.

34. Guzman ML, Rossi RM, Neelakantan S, Li X, Corbett CA, Hassane DC, et al. An orally bioavailable parthenolide analog selectively eradicates acute myelogenous leukemia stem and progenitor cells. Blood. 2007;110(13):4427-35.

35. Yip-Schneider MT, Wu H, Njoku V, Ralstin M, Holcomb B, Crooks PA, et al. Effect of celecoxib and the novel anti-cancer agent, dimethylamino-parthenolide, in a developmental model of pancreatic cancer. Pancreas. 2008;37(3):e45-53.

36. Shanmugam R, Kusumanchi P, Appaiah H, Cheng L, Crooks P, Neelakantan S, et al. A water soluble parthenolide analog suppresses in vivo tumor growth of two tobacco-associated cancers, lung and bladder cancer, by targeting NF-κB and generating reactive oxygen species. International journal of cancer. 2011;128(10):2481-94.

37. Shanmugam R, Kusumanchi P, Cheng L, Crooks P, Neelakantan S, Matthews W, et al. A water-soluble parthenolide analogue suppresses in vivo prostate cancer growth by targeting NFkappaB and generating reactive oxygen species. The Prostate. 2010;70(10):1074-86.

38. Holcomb BK, Yip-Schneider MT, Waters JA, Beane JD, Crooks PA, Schmidt CM. Dimethylamino parthenolide enhances the inhibitory effects of gemcitabine in human pancreatic

cancer cells. Journal of gastrointestinal surgery : official journal of the Society for Surgery of the Alimentary Tract. 2012;16(7):1333-40.

39. Morel KL, Ormsby RJ, Bezak E, Sweeney CJ, Sykes PJ. Parthenolide selectively sensitizes prostate tumor tissue to radiotherapy while protecting healthy tissues in vivo. Radiation Research. 2017;187(5).

40. Carlisi D, Buttitta G, Di Fiore R, Scerri C, Drago-Ferrante R, Vento R, Tesoriere. Parthenolide and DMAPT exert cytotoxic effects on breast caner stem-like cells by inducing oxidative stress, mitochondrial dysfunction and necrosis.

41. Isaacs WB, Carter BS, Ewing CM. Wild-type p53 suppresses growth of human prostate cancer cells containing mutant p53 alleles. Cancer research. 1991;51(17):4716-20.

42. Stone KR, Mickey DD, Wunderli H, Mickey GH, Paulson DF. Isolation of a human prostate carcinoma cell line (DU 145). International journal of cancer. 1978;21(3):274-81.

43. van Bokhoven A, Varella-Garcia M, Korch C, Johannes WU, Smith EE, Miller HL, et al. Molecular characterization of human prostate carcinoma cell lines. The Prostate. 2003;57(3):205-25.

44. Tepper CG, Gregg JP, Shi X-B, Vinall RL, Baron CA, Ryan PE, et al. Profiling of gene expression changes caused by p53 gain-of-function mutant alleles in prostate cancer cells. The Prostate. 2005;65(4):375-89.

45. Mendonca MS, Temples TM, Farrington DL, Bloch C. Evidence for a role of delayed death and genomic instability in radiation-induced neoplastic transformation of human hybrid cells. International journal of radiation biology. 1998;74(6):755-64.

46. Mendonca MS, Mayhugh BM, McDowell B, Chin-Sinex H, Smith ML, Dynlacht JR, et al. A radiation-induced acute apoptosis involving TP53 and BAX precedes the delayed apoptosis

and neoplastic transformation of CGL1 human hybrid cells. Radiation research. 2005;163(6):614-22.

47. Ma CM, Coffey CW, DeWerd LA, Liu C, Nath R, Seltzer SM, et al. AAPM protocol for 40-300 kV x-ray beam dosimetry in radiotherapy and radiobiology. Med Phys. 2001;28(6):868-93.

48. Turchan WT, Shapiro RH, Sevigny GV, Chin-Sinex H, Pruden B, Mendonca MS. Irradiated human endothelial progenitor cells induce bystander killing in human non-small cell lung and pancreatic cancer cells. Int J Radiat Biol. 2016;92(8):427-33.

49. Mendonca MS, Moriarty M, Mothersill C, Seymour C, Edington M, Ward JF, et al. Role of p53 and Delayed Apoptosis in Radiation-induced Neoplastic Transformation of Human Hybrid Cells2000. 496-9 p.

50. Estabrook NC, Chin-Sinex H, Borgmann AJ, Dhaemers RM, Shapiro RH, Gilley D, et al. Inhibition of NF-kappaB and DNA double-strand break repair by DMAPT sensitizes non-small-cell lung cancers to X-rays. Free Radic Biol Med. 2011;51(12):2249-58.

51. Olive PL, Banath JP. The comet assay: a method to measure DNA damage in individual cells. Nat Protoc. 2006;1(1):23-9.

52. Ostling O, Johanson KJ. Microelectrophoretic study of radiation-induced DNA damages in individual mammalian cells. Biochem Biophys Res Commun. 1984;123(1):291-8.

53. Iliakis G, Wang H, Perrault AR, Boecker W, Rosidi B, Windhofer F, et al. Mechanisms of DNA double strand break repair and chromosome aberration formation. Cytogenet Genome Res. 2004;104(1-4):14-20.

54. Olive PL. Impact of the comet assay in radiobiology. Mutat Res. 2009;681(1):13-23.

Figure 1 EMSA gel shift assays showing NF-κB p65/p50 heterodimer transcription factor binding to consensus promoter sequence in PC-3 cells (A, left panel) and DU145 cells (B, left panel) with and without treatment with DMAPT. Population doubling times of PC-3 cells (A, middle panel) and DU145 (B, middle panel) with and without treatment with DMAPT. Plating efficiency of PC-3 cells (A, right panel) and DU145 cells (B, right panel) with and without treatment with DMAPT. *$P < 0.05$, Student's *t* test.

Figure 2 (A and B, left panels) Annexin V flow cytometry results showing percentage DMAPT-treated and untreated control PC-3 (A) and DU145 (B) cells undergoing apoptosis. (A and B, right panels) Western blots for pro-apoptotic and anti-apoptotic proteins in DMAPT-treated and untreated control PC-3 (A) and DU145 (B) cells.

Figure 3 (A and B, left panels) EMSA showing NF-κB p65/p50 heterodimer transcription factor binding to consensus promoter sequence in untreated PC-3 (A) and DU145 (B) cells following treatment with 6 Gy of X-rays. (A and B, right panels) EMSA showing NF-κB p65/p50 heterodimer transcription factor binding to consensus promoter sequence in DMAPT-treated PC-3 (A) and DU145 (B) cells following treatment with 6 Gy of 160 kVp X-rays.

Figure 4 (Left, upper panel) Surviving fraction of PC-3 cells with and without treatment with DMAPT prior to receiving a single dose of either 0, 2, 4, or 6 Gy of X-rays. *$P < 0.05$, Student's

t test. (Right, upper panel) Surviving fraction of DU145 cells with and without treatment with DMAPT prior to receiving a single dose of 0, 3, 4, 5, 6 or 7 Gy of 160 kVp X-rays. **P* < 0.05, Student's *t* test. (Left, lower panel) Surviving fraction of PC-3 cells pre-treated or untreated with NAC with and without treatment with DMAPT prior to receiving a single dose of either 0, 2, 4, or 6 Gy of X-rays. **P* < 0.05, Student's *t* test. (Right, lower panel) Surviving fraction of PC-3 cells pre-treated or untreated with NAC with and without treatment with DMAPT prior to receiving a single dose of either 0, 2, 4, or 6 Gy of X-rays. **P* < 0.05, Student's *t* test.

Figure 5 DNA flow cytometry analysis after propidium iodide (PI) staining to determine the cell cycle distribution or percentage of cells in G1, S, and G2/M phase of PC-3 (A) and DU145 (B) cells that were treated with DMAPT versus cells untreated controls. No radiobiologically significant changes in cell cycle distribution were observed after treatment with DMAPT compared to controls.

Figure 6 (A, upper panels) Fractionation studies were performed to determine the surviving fraction of DMAPT-treated and untreated PC-3 (left) and DU145 (right) cells following treatment with 4 Gy of 160 kVp X-rays, either as a single fraction or as two fractions of 2 Gy, **P* < 0.01, Student's *t* test. (B, lower panels) PC-3 (left) and DU145 (right) cells were irradiated with 20 Gy of X-rays on ice with and without treatment with DMAPT and at various time post-irradiation were prepared for neutral comet assay. The comet olive tail moment for 50 individual cells from each treatment group are shown, **P* < 0.05, Student's *t* test.

Figure 7 Average relative tumor volume of PC-3 tumor xenografts following treatment with 6 Gy of X-rays and/or DMAPT. Athymic nude mice were injected with PC-3 cells on day 0 of the experiment. Xenografts in groups that received DMAPT were given 100 mg/kg DMAPT daily on days 8-14 post-implantation. Xenografts in groups that received radiation were irradiated with a 2 x 2 cm field of 6 Gy of 250 kVp X-rays on day 11 post-implantation. *$P < 0.05$, one-way ANOVA.

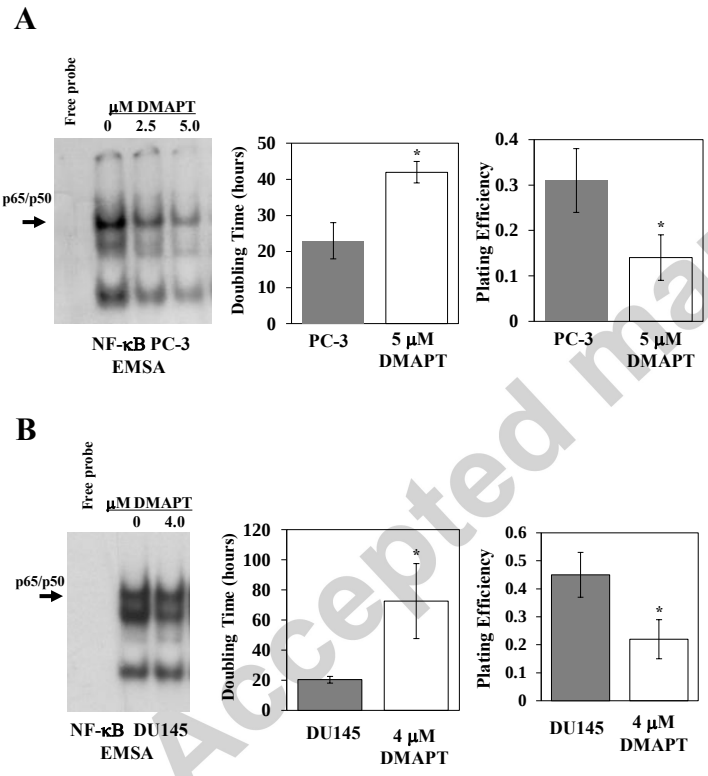

Figure 1

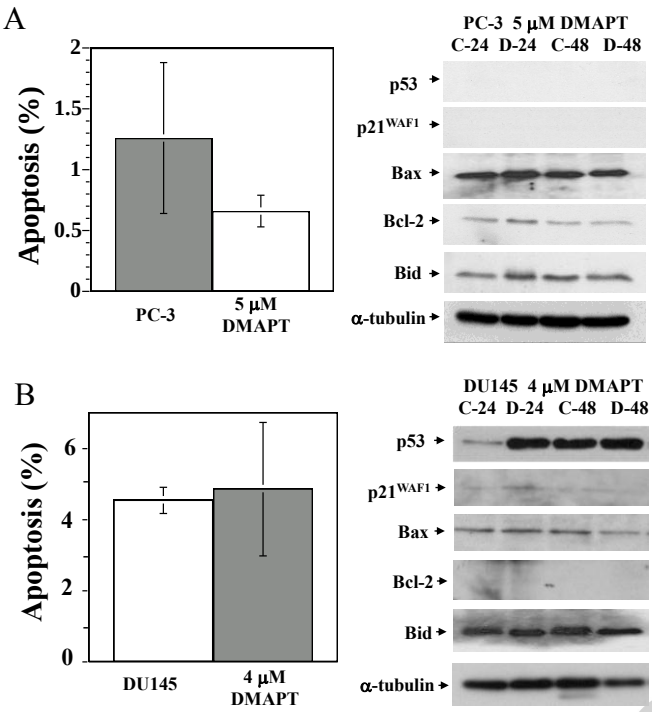

Figure 2

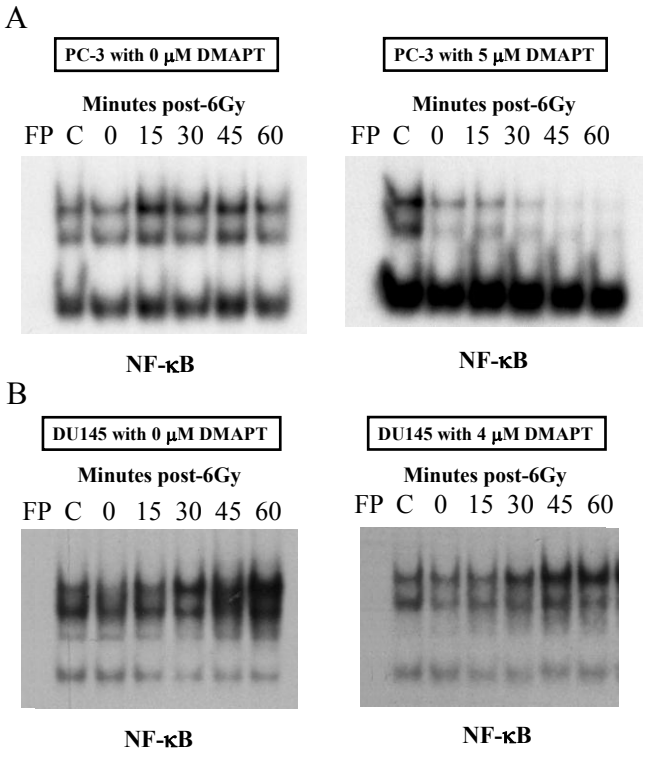

Figure 3

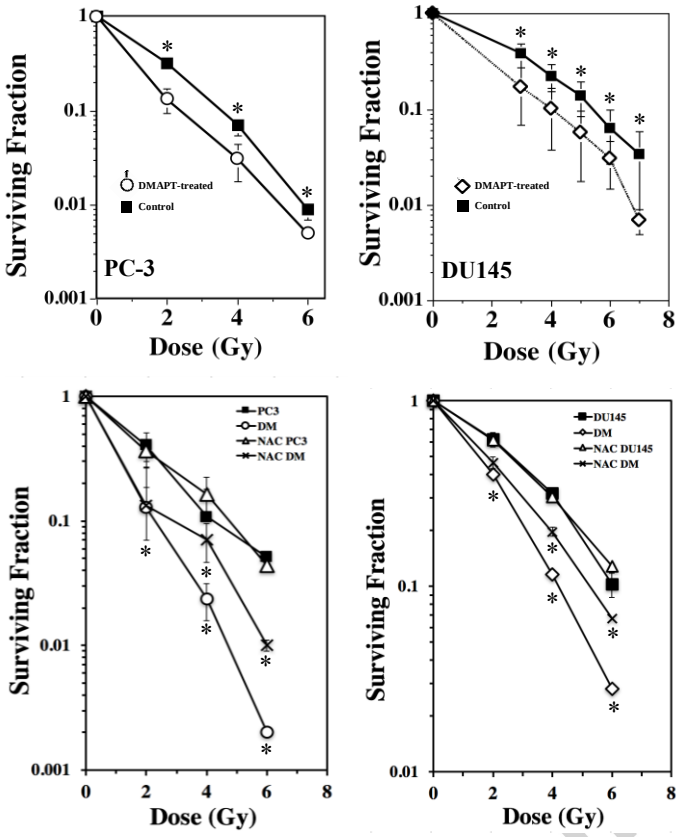

Figure 4 (revised)

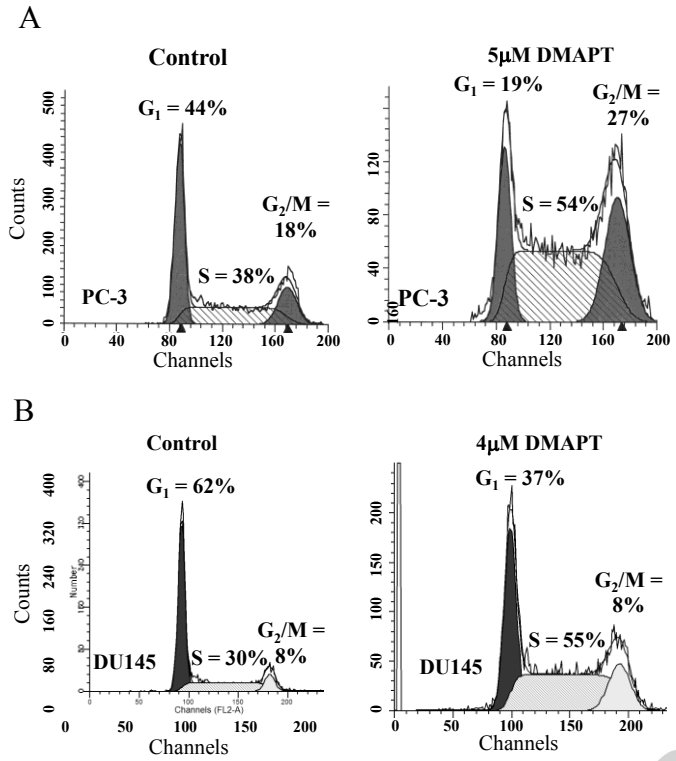

Figure 5

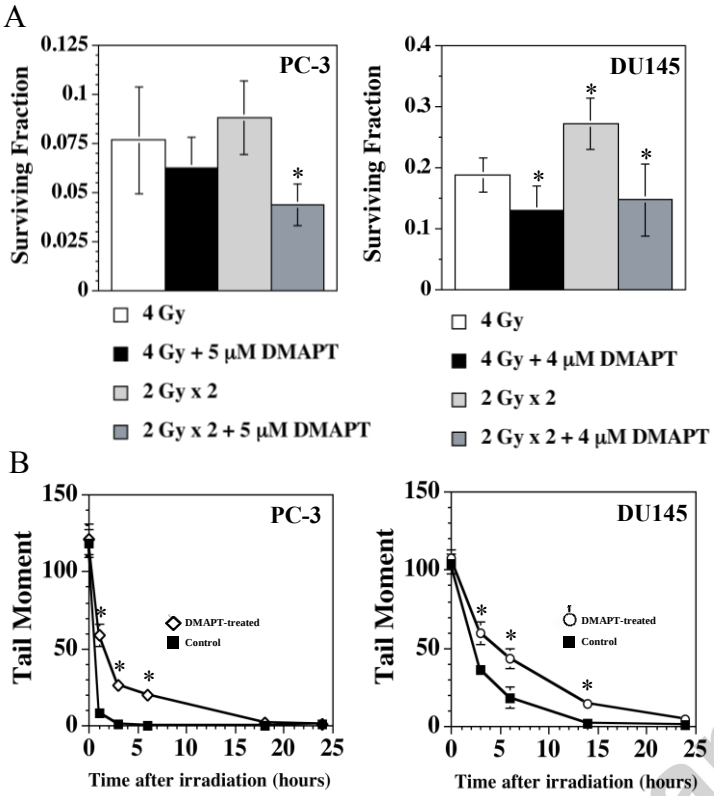

Figure 6

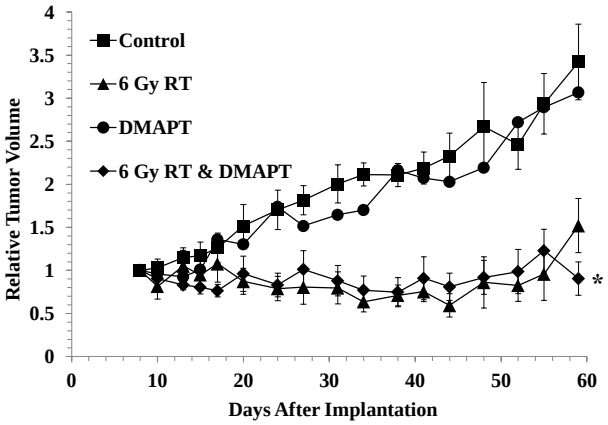

Figure 7

Highlights

- DMAPT inhibited constitutive and radiation-induced NF-κB binding activity.
- DMAPT slowed cell growth.
- DMAPT significantly increased single and fractionated X-ray induced cell killing in vitro.
- DMAPT inhibited X-ray induced DNA double strand break (DSB) repair in vitro.
- DMAPT enhanced X-ray induced anti-tumor activity in vivo.